



UNIVERSITY OF LEEDS

This is a repository copy of *Integration of Sentinel-1 Interferometry and GNSS Networks for Derivation of 3-D Surface Changes*.

White Rose Research Online URL for this paper:
<http://eprints.whiterose.ac.uk/162939/>

Version: Accepted Version

Article:

Bozsó, I, Bányai, L, Hooper, A orcid.org/0000-0003-4244-6652 et al. (2 more authors)
(2020) Integration of Sentinel-1 Interferometry and GNSS Networks for Derivation of 3-D Surface Changes. IEEE Geoscience and Remote Sensing Letters. ISSN 1545-598X

<https://doi.org/10.1109/LGRS.2020.2984917>

© 2020 IEEE. Personal use of this material is permitted. Permission from IEEE must be obtained for all other uses, in any current or future media, including reprinting/republishing this material for advertising or promotional purposes, creating new collective works, for resale or redistribution to servers or lists, or reuse of any copyrighted component of this work in other works. Uploaded in accordance with the publisher's self-archiving policy.

Reuse

Items deposited in White Rose Research Online are protected by copyright, with all rights reserved unless indicated otherwise. They may be downloaded and/or printed for private study, or other acts as permitted by national copyright laws. The publisher or other rights holders may allow further reproduction and re-use of the full text version. This is indicated by the licence information on the White Rose Research Online record for the item.

Takedown

If you consider content in White Rose Research Online to be in breach of UK law, please notify us by emailing eprints@whiterose.ac.uk including the URL of the record and the reason for the withdrawal request.



eprints@whiterose.ac.uk
<https://eprints.whiterose.ac.uk/>

Integration of Sentinel-1 Interferometry and GNSS Networks for Derivation of 3D Surface Changes

István Bozsó, László Banyai, Andrew Hooper, Senior Member, IEEE, Eszter Szűcs, and Viktor Wesztergom

Abstract—We present a new procedure and program system to integrate Sentinel-1 SAR interferometry and GNSS network observations to estimate 3-D surface changes caused by environmental processes.

The procedure is based on the integrated geodetic/geodynamic benchmarks, which are equipped with both ascending and descending corner reflectors. The results of sparse GNSS observations are interpolated using the ascending and descending line-of-sight changes provided by the Sentinel-1 mission every six days. The data integration is carried out using a Kalman-filter where North, East and Up (vertical) coordinates and their instantaneous velocities are estimated and updated by GNSS derived data. The North components are essentially provided by the GNSS observations alone.

The procedure was developed and successfully tested on landslide areas in Hungary.

Index Terms—Sentinel-1, InSAR, GNSS, Kalman-filter

I. INTRODUCTION

ALTHOUGH there are well tested procedures to estimate the movements in azimuth directions using SAR (Synthetic Aperture Radar) interferometry [1,2,3], their accuracy is still significantly worse than the accuracy of the line-of-sight (LOS) changes estimated by traditional InSAR techniques. Since ascending and descending LOS displacements are barely sensitive to displacements in the North direction, data fusion with GNSS techniques is the preferable choice to derive 3-D surface changes [4].

To this end, we have developed the ISIGN (Integration of Sentinel-1 Interferometry and GNSS Networks) procedure and software package, which is based on the application of integrated geodetic/geodynamic benchmarks (IBs). These IBs

This paragraph of the first footnote will contain the date on which you submitted your paper for review.

This work was supported in part by European Space Agency, Plan for European Cooperating States (ESA PECS) through a project under grant 4000114846/15/NL/NDe, in part by the National Excellence Program under Grant 2018-1.2.1-NKP-2018-00007.

I. Bozsó, L. Banyai, E. Szűcs, and V. Wesztergom are with the Geodetic and Geophysical Institute, CSFK, 9400 Sopron, Hungary (e-mail: bozso.istvan@csfk.mta.hu; banyai.laszlo@csfk.mta.hu; szucs.eszter@csfk.mta.hu; wesztergom.viktor@csfk.mta.hu).

A. Hooper is with the COMET, School of Earth and Environment, University of Leeds, Leeds LS2 9JT, U.K. (e-mail: a.hooper@leeds.ac.uk).

are equipped with truncated trihedral triangle corner reflectors oriented toward ascending and descending satellite directions together with GNSS reference adapters and other marks to investigate the tilt of the reinforced concrete basement (Fig. 1). The mechanical design, electromagnetic investigations and practical test of the IBs are described in [5].

In this letter the ISIGN procedure is introduced, which is designed to interpolate the results of sparse GNSS (Global Navigation Satellite System) epoch measurements with Sentinel-1 ascending and descending LOS changes available every sixth days using the method of a Kalman-filtering approach.

The role of GNSS measurements is threefold: they help the identification of the pixels dominated by the signal reflected by IBs; they indicate unwrapping errors or missing phase cycles; and they provide information on movements in the North direction. The frequency of GNSS measurements depends on the movement rate of the investigated phenomenon. The IBs can be measured as members of local or permanent GNSS (Global Navigation Satellite Systems) networks. The GNSS accuracy of North, East and Up (vertical) components between the stable and moving IBs should be comparable or even better than the LOS displacement accuracy derived from InSAR processing.

Our main experiences during the development of the methodology and the application of it on recent landslide test networks in Hungary are also summarized.

II. ISIGN METHOD AND PROGRAM SYSTEM

The Gamma DIFF&GEO software package [6] is used to provide georeferenced differential interferograms, coherence and normalised reflected power images from raw Sentinel-1 SLC (Single Look Complex) data files. The StaMPS (Stanford Method for Persistent Scatterers) software [7] is then applied to estimate the LOS time series of selected pixels without imposing a preliminary deformation model.

The differential interferograms are wrapped, i.e. do not contain the full waves of the surface deformation. The unwrapping (the estimation of missing waves) is the most crucial and not evident step of the InSAR processing. One of the significant limiting factors is the distance between the selected pixels, which should be less than 3-4 km [8] to avoid the undersampling of the interferometric phase.

StaMPS is designed to identify and to unwrap the phase of dense scatterers (in time and space) which can help the unwrapping if IBs are far from the ideal distance.

As an alternative solution the LOS time series can be derived directly from the Gamma differential interferograms using 1-D unwrapping in time if the nearby IBs behave as persistent scatterers. The results then become the input of the ISIGN procedure.

The program system consists of three main blocks comprised of fourteen modules.

A. Network maintenance block

In this block the geometric parameters (azimuth and incidence angle) of the LOS vectors are computed for the individual IBs using the method of closest approach. In the closest approach position, calculated iteratively from satellite orbit data and IB coordinates, the satellite velocity vector is perpendicular to the LOS vector defined by the scalar product:

$$\mathbf{v}_{SAT}(t)(\mathbf{x}_{SAT}(t) - \mathbf{x}_{IB}) = 0, \quad (1)$$

where \mathbf{x}_{IB} is the known position vector of IB, \mathbf{v}_{SAT} is the velocity and \mathbf{x}_{SAT} is the position vector of satellite, they are the function of time t .

The computed parameters are used for the orientation of the reflectors. The geometric parameters of the reference IB on master images are also used in the Kalman-filtering procedure.

Precise geodetic levelling and total station measurements are carried out regularly to determine the relative positions of the two-phase centers and other four geodetic marks with respect to the GNSS reference mark of IBs [5]. The changes between two measurements are used to estimate the tilt of the IBs, which may be significant, e.g. in the case of landslide investigations. If two successive geodetic and GNSS measurements are available, the LOS differences between the two epochs and between the reference and other IBs are computed and corrected by the tilt of the IBs for both ascending and descending directions.

B. LOS preparation block

In this block candidate pixels, which may be dominated by our IBs, are selected using a predefined area for all normalised power images. The pixels, in which the average normalised power values are local maxima and larger than a predefined threshold, are selected as IBs candidates.

The automatic identification of the candidates as IBs is carried out using combination and permutation calculations: n number of candidates are selected in all combinations and the combinations are permuted in all order; the distances between the selected pixels and the n number of IBs (measured by GNSS) are computed; the set of pixels with minimum distance dispersion are identified as IBs.

The automatic identification cannot always guarantee the right solution if the nearby pixels behave like IBs. In this case the graphic selection tool can be used to filter the candidates, to define the pixel-IB pairs or control the automatic solution.

Using the phase noise, StaMPS independently selects pixels dominated by persistent scatterers, which should include the IBs. If the IBs are not included, the identification and/or

StaMPS computations are repeated with different parameters.

C. LOS processing block

In the first step of this block: 1) the LOS time series of the identified pixels are computed from the StaMPS ASCII result files, alternatively the time series can also be calculated directly from the Gamma interferograms and converted to LOS displacement values after the 1-D unwrapping in time. 2) LOS time series differences are calculated between the reference and other IBs.

In both cases the applied unwrapping methods do not guarantee an error-free solution. Computing the LOS values from GNSS coordinate changes allows us to improve the unwrapping manually and to estimate the locations of probable missing phase cycles.

Stepwise quadratic interpolation is used to interpolate the ascending LOS data in the epoch of descending acquisitions and vice versa, together with the epochs of the starting and closing (if exist) GNSS network observations.

Since only slow surface deformation can be estimated by InSAR techniques, the applied dynamic model of the Kalman-filter contains only positions and respective velocities in North (n), East (e) and Up (u) components.

The dynamic state equation is:

$$\mathbf{x}'_i = \begin{bmatrix} n'_i \\ e'_i \\ u'_i \\ v'_{n_i} \\ v'_{e_i} \\ v'_{u_i} \end{bmatrix} = \begin{bmatrix} 1 & 0 & 0 & \Delta t & 0 & 0 \\ 0 & 1 & 0 & 0 & \Delta t & 0 \\ 0 & 0 & 1 & 0 & 0 & \Delta t \\ 0 & 0 & 0 & 1 & 0 & 0 \\ 0 & 0 & 0 & 0 & 1 & 0 \\ 0 & 0 & 0 & 0 & 0 & 1 \end{bmatrix} \begin{bmatrix} \hat{n}_{i-1} \\ \hat{e}_{i-1} \\ \hat{u}_{i-1} \\ \hat{v}_{n_{i-1}} \\ \hat{v}_{e_{i-1}} \\ \hat{v}_{u_{i-1}} \end{bmatrix} = \mathbf{T} \hat{\mathbf{x}}_{i-1}, \quad (2)$$

where \mathbf{x}'_i is the predicted, $\hat{\mathbf{x}}_{i-1}$ the previous filtered vector of parameters, \mathbf{T} is the transfer matrix and $\Delta t = (t_i - t_{i-1})$ is a time difference between the two epochs. The LOS observation equation:

$$\mathbf{b} = \mathbf{A} \mathbf{x}'_i, \quad \mathbf{b} = \begin{bmatrix} l_A \\ l_D \end{bmatrix} \quad (3)$$

$$\mathbf{A} = \begin{bmatrix} -\cos \alpha_A \sin \zeta_A & -\sin \alpha_A \sin \zeta_A & \cos \zeta_A & 0 & 0 & 0 \\ -\cos \alpha_D \sin \zeta_D & -\sin \alpha_D \sin \zeta_D & \cos \zeta_D & 0 & 0 & 0 \end{bmatrix}$$

where l is the LOS values in epoch i , α is the satellite-IB azimuth and ζ is the IB-satellite incidence angle computed in topocentric coordinate system attached to reference IB and master image, subscripts A and D denote ascending and descending satellite passes respectively. The observation equation is derived in [4].

The steps of combined solution are:

$$\begin{aligned} \mathbf{x}'_i &= \mathbf{T} \hat{\mathbf{x}}_{i-1} \\ \mathbf{Q}_{x_i} &= \mathbf{T} \mathbf{Q}_{\hat{\mathbf{x}}_{i-1}} \mathbf{T}^t + \mathbf{Q}_x \\ \mathbf{K} &= \mathbf{Q}_{x_i} \mathbf{A}^t (\mathbf{Q}_b + \mathbf{A} \mathbf{Q}_{x_i} \mathbf{A}^t)^{-1} \\ \hat{\mathbf{x}}_i &= \mathbf{x}'_i + \mathbf{K}(\mathbf{b} - \mathbf{A} \mathbf{x}'_i) \\ \mathbf{Q}_{\hat{\mathbf{x}}_i} &= (\mathbf{I} - \mathbf{K} \mathbf{A}) \mathbf{Q}_{x_i} \end{aligned} \quad (4)$$

where \mathbf{K} is the Kalman or gain matrix, \mathbf{Q}_x is the variance matrix of the model uncertainty, \mathbf{Q}_b is the variance matrix of the LOS observations, \mathbf{Q}_{x_i} is the variance matrix of predicted and $\mathbf{Q}_{\hat{\mathbf{x}}_i}$ is the variance matrix of filtered parameters.

The coordinate changes estimated by this procedure will differ from the GNSS derived changes in the closing epoch. Since ordinary initial velocities can be chosen in the initial epoch, the estimated traverse may be rotated, and the scale of ASC and DSC LOS values may be different, as well. The analogy of the free traversing in traditional surveying provided the proper solution. If the velocity updates are computed by

$$\begin{aligned} v_{n_0} &= \frac{n_{GNSS_c} - GNSS_0}{\Delta t} \\ v_{e_0} &= \frac{e_{GNSS_c} - GNSS_0}{\Delta t} \\ v_{u_0} &= \frac{u_{GNSS_c} - GNSS_0}{\Delta t} \end{aligned} \quad (5)$$

using the coordinate changes from GNSS measurements and additionally the ASC and DSC LOS series are rescaled using the GNSS derived LOS values in the last epoch, the best fitting results can be provided in least squares sense. If the rescaled LOS values would be treated as errorless quantities the three curves would coincide exactly with the last GNSS solution, however, in this case there would be no filtering at all. If we suppose that the GNSS measurements are more accurate the residual coordinate differences can be handled by additional rescaling, too

The adopted Kalman filter is described exhaustively in [9,10].

The predicted positions are continuously updated by simultaneous ascending and descending LOS displacement data. In the initial step, zero displacements and velocities can be chosen, unless we have some preliminary information. In this case the 3D coordinates will differ from the GNSS derived coordinates in the closing GNSS epoch, especially in the case of the North component.

When the closing GNSS positions are available, the full solution can be updated using the GNSS derived average initial velocities, the rescaled ascending and descending LOS series, which provides the best fitting solution in a least squares sense. The residual differences can be additionally rescaled in the third step, if the GNSS measurements provide more accurate values than the InSAR derived values.

The main steps of the two possible solutions are summarised in Fig. 2.

The alternative procedure is less time consuming, but there are significant theoretical differences between the two concepts. StaMPS applies sophisticated filtering methods to remove various error sources, while the alternative method (deriving LOS displacement time-series from Gamma interferograms) only applies a differencing technique. Consequently, the alternative method can be used only in local cases, where the IBs are close enough to each other.

The use of StaMPS is preferable in larger areas, if there is a sufficient number of “natural” persistent and/or distributed scatterers between the IBs, which makes unwrapping and the separation of different error sources possible.

III. FIRST EXPERIENCES DURING ISIGN DEVELOPMENT

ISIGN was developed using our experiences from the data processing of three practical test networks established on landslide areas in Hungary. The main results are summarised

in this chapter.

Fig. 3 presents the IB candidates in the village of Kulcs, where the GNSS measured reference positions of IBs are indicated by crosses. The distance dispersion between the identified candidate pixels and known IB positions in both ascending and descending cases are ~10-15 m, which is in accordance with the single look pixel size.

In the case of A4, a larger difference was found between ascending and descending candidate pair. This point was established in an area in which a large amount of mass movement occurred during the last landslide, which is not corrected in the SRTM DEM (Shuttle Radar Topography Mission, Digital Elevation Model) model that was used.

Near to A1 there is another ascending and descending candidate pair, which is a reflection from a nearby metallic container house. This indicates the necessary field control of the numeric identification, since “natural” scatterers may provide smaller distance dispersion.

There are only three “natural” ascending and descending pairs (only one on the moving area), which can be used to estimate East and Up movements despite the presence of several buildings. This demonstrates the usefulness of the IBs.

The manual unwrapping procedure needed to correct the missing cycles is demonstrated in the case of the Dunaszekcső network (Fig. 4). The relative LOS curve properly indicates the general trend, but three half cycles are missing, that are needed to fit the LOS time series to the GNSS data. There is one short reverse period, where the trend shows controversial movements (indicated in Fig. 4), which is not possible in the case of this landslide. This is a consequence of different movement rate and the 6-day repeat cycle of the Sentinel-1 mission leading to missing cycles. The earlier geodetic and GNSS measurements [11] prove that there were faster periods that cannot be sampled with a 6-day repeat cycle.

One ideal solution is given in Fig. 5 and 6, where manual interactions were not necessary (Kulcs network). The LOS time series from StaMPS and the alternative approach are practically the same, and differ from the GNSS derived values by only a few millimetres (Fig. 5). This is a consequence of a small distance between IBs. The result of the Kalman-filtering (Fig. 6) shows that the North component is basically provided by GNSS measurements, however the magnitudes of the North and East components are very similar.

The a priori standard deviations of InSAR and GNSS derived LOS values were assumed to be 2 mm, the resulting North, East and Up standard deviations are 16 mm, 2 mm and 3 mm respectively.

IV. CONCLUSIONS

The ISIGN procedure and software system proved to be a useful approach for the estimation of 3-D surface changes using integrated geodetic/geodynamic benchmarks.

The data processing of Gamma GEO&DIFF and StaMPS software were integrated into the ISIGN processing chain. The LOS time series can be provided by StaMPS, or directly derived from the Gamma differential interferograms. In the case of close IBs (local networks) the resulting curves are very

similar and the comparison of the two solutions may be advantageous, since they apply different unwrapping and error filtering methods. StaMPS is the preferable solution in the case of larger networks, where a good distribution of “natural” scatters is also required.

If single look images are processed, which are preferable in the case of IBs, the distances between the identified georeferenced pixels and GNSS measured positions are typically 10-15 m. If the DEM models used have larger errors, these distances may be larger.

For the correction of missing cycles, the GNSS derived LOS changes and the knowledge of the investigated phenomenon is also required.

During the Kalman-filtering the North component basically originates from GNSS measurements. Moreover, this knowledge may be very important for the practical interpretation of the 3D movements.

Although the recent version of ISIGN can be used very efficiently, there are several possibilities to improve the procedure (e.g. rigorous filtering of images, use of precise satellite orbits, advanced LOS interpolation with smoothing and more convenient manual unwrapping).

REFERENCES

- [1] N. D. B. Bechor and H. A. Zebker, “Measuring two-dimensional movements using a single InSAR pair,” *Geophys. Res. Lett.*, 33 (16) pp. 5. 2006.
- [2] E. Erten, A. Reigber and O. Hellwich, “Generation of three-dimensional deformation maps from InSAR data using spectral diversity techniques,” *ISPRS J. Photogramm. Remote Sens.* 65 (4) pp 388-394. 2010.
- [3] A. Hooper and K. Spaans, “Sentinel-1 along-track InSAR for global strain rate estimation,” *Fringe International Workshop*, Alto University, Helsinki, Finland. 2017.
- [4] L. Bányai, E. Szűcs and V. Wesztergom, “Geometric features of LOS data derived by SAR PSI technologies and the three-dimensional data fusion,” *Acta Geod. Geoph.* 52(3), pp 421–436, 2016.
- [5] L. Bányai, L. Nagy, A. Hooper, E. Szűcs, I. Bozsó and V. Wesztergom, “Investigation of Integrated Twin Corner Reflectors Designed for 3-D InSAR Applications,” *IEEE GRSL 2019*. DOI 10.1109/LGRS.2019.2939675.
- [6] C. Werner, U. Wegmüller, T. Strozzi and A. Wiesmann, “Gamma SAR and Interferometric Processing Software,” *ERS - ENVISAT Symposium*, Gothenburg, Sweden, 16-20 Oct. pp. 9, 2000.
- [7] A. Hooper, D. Bekaert, K. Spanns and M. Arikan, “Recent advances in SAR interferometry time series analysis for measuring crustal deformations,” *Tectonophysics*, 1-13, pp. 514-517, 2012.
- [8] A. Ferretti, “Satellite InSAR Data”, *EAGE Publications* bv., p. 159., 2014.
- [9] G. Strang and K. Borre, “Linear algebra, geodesy, and GPS,” p. 624 *Wellesley–Cambridge Press*, Wellesley, 1997
- [10] P. J. G. Teunissen, “Dynamic data processing - recursive least-squares”. *Series on Mathematical Geodesy and Positioning*, p. 241. *Delft University Press*, 2001.
- [11] L. Bányai, Gy. Mentés, G. Újvári, M. Kovács, Z. Czap, K. Gribovszki and G. Papp, “Recurrent landsliding of a high bank at Dunaszekcső, Hungary: Geodetic deformation monitoring and finite element modeling,” *Geomorphology*, 210, pp. 1-13, 2014.



Fig. 1. Manufactured integrated geodetic/geodynamic benchmarks

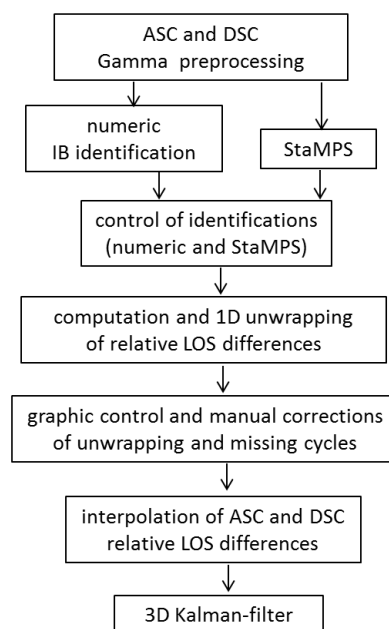


Fig. 2. Flowchart of the main processing steps.

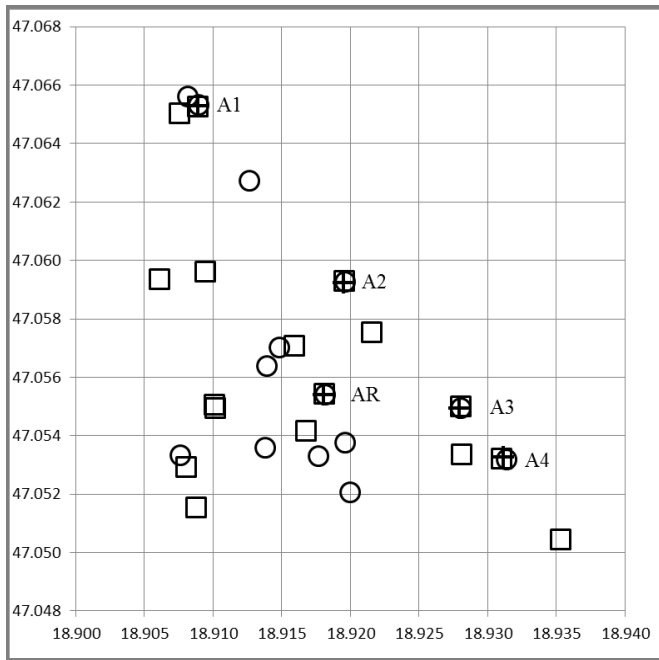


Fig. 3. The candidates and identified ascending (circle) and descending (square) pixels with GNSS positions (cross) plotted in geographic coordinate system (degree).

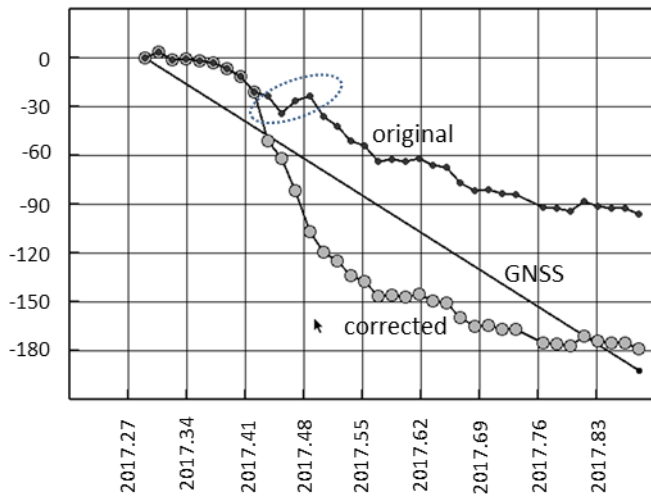


Fig. 4. Manual unwrapping of LOS series (mm).

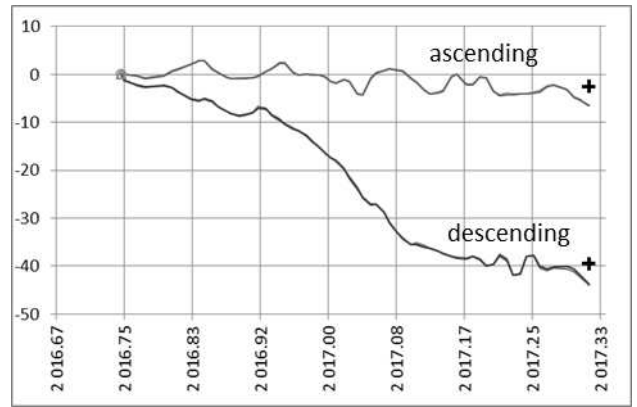


Fig. 5. Interpolated LOS series (mm), the GNSS derived values are plotted with crosses.

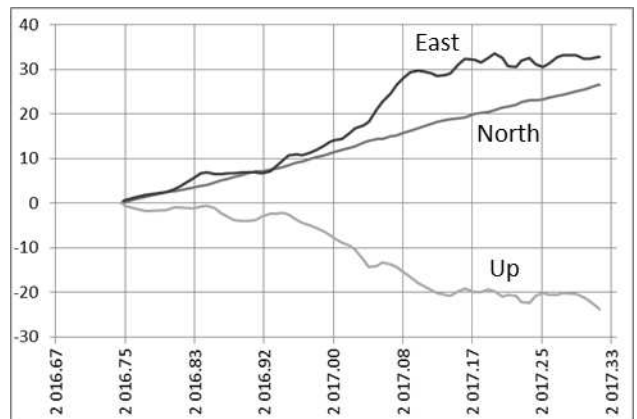


Fig. 6. The estimated coordinate changes (mm) fitted to the GNSS results.